Synthesis, crystal structure and magnetic properties of the cobalt(II) chain $[Co(bipym)(H_2O)_2](NO_3)_2$ and the dinuclear compounds $[Co_2(bipym)_3(H_2O)_4](NO_3)_4 \cdot 2H_2O$ and $[Co_2(bipym)_3(H_2O)_2(SO_4)_2] \cdot 12H_2O$

Giovanni De Munno,*[a] Teresa Poerio,[a] Miguel Julve,*†[b] Francesc Lloret[b] and Guillaume Viau[b]

[a] *Dipartimento di Chimica, Università degli Studi della Calabria, 87030 Arcavacata di Rende (Cosenza), Italy*
[b] *Departament de Química Inorgànica, Facultat de Química de la Universitat de València, Dr. Moliner 50, 46100 Burjassot (València), Spain*

Three new cobalt(II) complexes of formula $[Co(bipym)(H_2O)_2](NO_3)_2$ (**1**), $[Co_2(bipym)_3(H_2O)_4](NO_3)_4 \cdot 2H_2O$ (**2**) and $[Co_2(bipym)_3(H_2O)_2(SO_4)_2] \cdot 12H_2O$ (**3**) (bipym = 2,2′-bipyrimidine) have been synthesized and characterized by single-crystal X-ray diffraction. The structure of **1** consists of cationic chains of cobalt(II) ions bridged by bis(chelating) bipym whereas those of **2** and **3** are made up of dinuclear entities containing both chelating and bis(chelating) bipym ligands. The metal atom in this family is bound to four bipym nitrogen atoms belonging to two bipym groups (**1**–**3**) and to two *cis* oxygen atoms belonging either to water molecules (**1** and **2**) or to water and monodentate sulfate (**3**), to build a distorted CoN_4O_2 octahedral environment. A crystallographically imposed inversion center is located halfway between the two pyrimidyl rings of the bridging bipym. The metal–metal separation across bridging bipym varies between 5.736(2) and 5.808(2) Å. The study of the magnetic properties of **1**–**3** in the temperature range 2.5–290 K reveals the occurrence of antiferromagnetic coupling with susceptibility maxima at 18 (**1**), 14 (**2**) and 13.5 K (**3**). Fits of the magnetic data through the Lines and Ising models were carried out and the results compared and discussed.

Synthèse, structure et propriétés magnétiques de la chaîne de cobalt(II) $[Co(bipym)(H_2O)_2](NO_3)_2$ et des complexes binucléaires $[Co_2(bipym)_3(H_2O)_4](NO_3)_4 \cdot 2H_2O$ et $[Co_2(bipym)_3(H_2O)_2(SO_4)_2] \cdot 12H_2O$. Trois nouveaux complexes de cobalt(II) de formule $[Co(bipym)(H_2O)_2](NO_3)_2$ (**1**), $[Co_2(bipym)_3(H_2O)_4](NO_3)_4 \cdot 2H_2O$ (**2**) et $[Co_2(bipym)_3(H_2O)_2(SO_4)_2] \cdot 12H_2O$ (**3**) (bipym = 2,2′-bipyrimidine) ont été synthetisés et caractérisés par diffraction des rayons X sur monocristal. Le premier composé présente une structure en chaîne où les atomes de cobalt sont pontés par la bipym agissant comme coordinat bis(bidente) tandis que les structures des deux autres complexes sont dimériques avec la bipym bis(bidente) et bidente. L'atome métallique dans cette famille est lié à quatre atomes d'azote de deux coordinats bipym (**1**–**3**) et à deux atomes d'oxygène en *cis* soit de deux molécules d'eau (**1** et **2**) ou d'une molécule d'eau et d'un groupement sulphate (**3**) qui créent un environnement CoN_4O_2 octaédrique distordu. Un centre d'inversion cristallographique se trouve au point moyen de la liaison entre les deux anneaux pyrimidine de la bipym pontante. La distance entre les atomes métalliques à travers la bipym varie entre 5.736(2) et 5.808(2) Å. L'étude des propriétés magnétiques des complexes **1**–**3** en fonction de la température de 290 K à 2.5 K montre que les spins des ions métalliques sont couplés antiferromagnétiquement; les courbes de la susceptibilité magnétique présentent un maximum à 18 (**1**), 14 (**2**) et 13.5 K (**3**). Les valeurs du paramètre d'échange obtenues par ajustement des données magnétiques à l'aide des expressions issues des modèles de Lines et Ising sont comparées et discutées.

2,2′-Bipyrimidine (hereafter noted bipym) is a bis(α-diimine)-type ligand, which can exhibit chelating and bis(chelating) coordination modes in its metal complexes.[1,2] This molecule has a remarkable efficiency to transmit electronic interactions between metal ions that are separated by more than 5.5 Å through bridging bipym. The upper limit known for the magnetic interaction is -236 cm^{-1} (singlet–triplet energy gap) in the compound of formula $[Cu_2(bipym)Cl_4]$.[3] The most relevant magneto-structural results that have been obtained with its complexes with first-row transition metal ions are: (i) the preparation of nuclearity-tailored polynuclear compounds by using different metal to bipym molar ratios and suitable coligands, (ii) a rational strategy in designing homometallic chains exhibiting regular alternating ferro- and antiferromagnetic interactions and (iii) the design of new honeycomb-layered materials with alternating magnetic interactions. The best example to illustrate the first point is represented by the Mn^{II}–bipym system: the reaction of manganese(II) salts and bipym in aqueous solution allowed the preparation of mononuclear species for the higher values of the metal to ligand molar ratio $\{[Mn(bipym)_3](ClO_4)_2$ and $[Mn(bipym)_2(H_2O)_2](ClO_4)_2\}$,[4,5] whereas dinuclear $\{[Mn_2(bipym)(H_2O)_4](SO_4)_2$, $[Mn_2(bipym)_3(NCS)_4]$ and $[Mn_2(bipym)_3(NCSe)_4]\}$,[6,7] chain $\{[Mn(bipym)(NO_3)_2]$ and $[Mn(bipym)(NCO)_2]\}$[5,8] and two- and three-dimensional $\{[Mn_2(bipym)(N_3)_4]\}$[9] compounds were obtained for lower Mn^{II} : bipym molar ratios. Dealing with

† E-mail: miguel.julve@uv.es; Fax: (34) 6 3864322.

Table 1 Crystallographic data and structure refinement for complexes **1**–**3**

Compound	**1**	**2**	**3**
Empirical formula	$C_8H_{10}CoN_6O_8$	$C_{24}H_{30}Co_2N_{16}O_{18}$	$C_{24}H_{46}Co_2N_{12}O_{22}S_2$
Formula weight	377.2	948.5	1036.7
Crystal system	Monoclinic	Triclinic	Monoclinic
Space group	$P2_1/c$	$P\bar{1}$	$P2_1/n$
a/Å	10.417(2)	9.890(3)	12.830(3)
b/Å	15.204(3)	10.292(4)	10.128(2)
c/Å	8.558(2)	10.524(3)	16.133(4)
α/°		96.37(3)	
β/°	92.95(2)	113.83(2)	91.38(2)
γ/°		106.78(3)	
U/Å^3	1358.4(5)	905.9(5)	2095.8(8)
Z	4	1	2
D_c/g cm^{-3}	1.844	1.739	1.643
F(000)	764	484	1072
$\mu_{MoK\alpha}$/cm^{-1}	13.2	10.2	16.4
Index ranges	$-13 \leqslant h \leqslant 8$	$0 \leqslant h \leqslant 12$	$0 \leqslant h \leqslant 16$
	$0 \leqslant k \leqslant 19$	$-13 \leqslant k \leqslant 12$	$0 \leqslant k \leqslant 12$
	$0 \leqslant l \leqslant 10$	$-13 \leqslant l \leqslant 12$	$-20 \leqslant l \leqslant 20$
Max./min. transmission	0.899/0.606	0.855/0.737	0.718/0.688
No. refl. collected	3383	4291	5303
No. unique reflections	2985	3989	4591
R_{int}	0.014	0.025	0.012
No. obsd. reflections, N_o $[I > 3\sigma(I)]$	1573	3501	3310
Weighting scheme, w^{-1}	$\sigma^2(F_0) + 0.0011F_0^2$	$\sigma^2(F_0) + 0.0016F_0^2$	$\sigma^2(F_0) + 0.0003F_0^2$
No. of parameters refined, N_p	217	289	322
Largest and mean Δ/σ	0.011, 0.001	0.004, 0.000	0.002, 0.000
Largest diff. peak/hole (e Å^{-3})	0.59/−0.54	0.69/−0.47	0.32/−0.40
R [a]	0.055	0.034	0.035
R_w [b]	0.057	0.040	0.037
Goodness-of-fit[c]	1.33	1.20	1.65

[a] $R = \sum(\|F_o\| - \|F_c\|)/\sum|F_o|$. [b] $R_w = [\sum w(\|F_o\| - \|F_c\|)^2/\sum wF_o^2]^{1/2}$. [c] G.o.f. $= [\sum(\|F_o\| - \|F_c\|)^2/(N_o - N_p)]^{1/2}$.

the second point, the polymerization through bipym of the di-μ-hydroxocopper(II) complex $[Cu_2(bipym)_2(H_2O)_2(OH)_2(NO_3)_2]\cdot 4H_2O$ yielded copper(II) chains exhibiting a regular alternation of bipym and double hydroxo bridges, which mediate antiferro- and ferromagnetic interactions, respectively.[10] Finally, as far as the third point is concerned, sheet-like polymers exhibiting alternating antiferromagnetic (through bipym and oxalato bridges)[6,11] and antiferro-ferromagnetic (through bipym and double end-on azido bridges)[9,12] interactions have been reported. The lack of a suitable theoretical model has precluded the analysis of the magnetic data of these interesting two-dimensional compounds. The preparation and magneto-structural characterization of simpler and lower dimensionality systems is crucial in order to get the values of the exchange coupling constants involved in the higher dimensionality systems.

In the present work we report the preparation as well as the structural and magnetic characterization of the first bipym-bridged Co^{II} chain $[Co(bipym)(H_2O)_2](NO_3)_2$ (**1**) together with those of the two related Co^{II} dimers $[Co_2(bipym)_3(H_2O)_4](NO_3)_4\cdot 2H_2O$ (**2**) and $[Co_2(bipym)_3(H_2O)_2(SO_4)_2]\cdot 12H_2O$ (**3**).

Experimental

General

Cobalt(II) nitrate hexahydrate, cobalt(II) sulfate heptahydrate and 2,2′-bipyrimidine were purchased from commercial sources and used as received. Elemental analyses (C, H, N) were performed by the Microanalytical Service of the Università degli Studi della Calabria (Italy).

The IR spectra were obtained with a Perkin–Elmer 1750 FTIR spectrophotometer on KBr pellets in the 4000–400 cm^{-1} region. The magnetic susceptibility measurements on polycrystalline samples of the complexes **1**–**3** were carried out in the temperature range 2.5–290 K with a MS03 SQUID magnetometer operating at 1 T. $(NH_4)_2Mn(SO_4)_2\cdot 6H_2O$ was used as a calibrant. Diamagnetic corrections were estimated from Pascal's constants[13] as -181×10^{-6} (**1**), -493×10^{-6} (**2**) and -501×10^{-6} (**3**) cm^3 mol^{-1}.

Preparations

$[Co(bipym)(H_2O)_2](NO_3)_2$ (**1**). Prismatic orange-pink crystals of **1** were obtained by slow evaporation at room temperature of an orange aqueous solution containing stoichiometric amounts of $Co(NO_3)_2\cdot 6H_2O$ (1 mmol) and bipym (1 mmol). The solid product was filtered off and washed with ethanol. Anal. calcd for $C_8H_{10}CoN_6O_8$: C, 25.48; H, 2.67; N, 22.28. Found: C, 25.36; H, 2.59; N, 22.34%.

$[Co_2(bipym)_3(H_2O)_4](NO_3)_4\cdot 2H_2O$ (**2**) and $[Co_2(bipym)_3(H_2O)_2(SO_4)_2]\cdot 12H_2O$ (**3**). Prismatic orange-yellow crystals of **2** and orange ones of **3** were obtained by slow evaporation at room temperature of orange aqueous solutions containing nonstoichiometric amounts of $Co(NO_3)_2\cdot 6H_2O$ or $Co(SO_4)_2\cdot 7H_2O$ (1 mmol) and bipym (1.75 mmol). The crystals were filtered off and washed with ethanol. Anal. calcd for $C_{24}H_{30}Co_2N_{16}O_{18}$ (**2**): C, 30.39; H, 3.19; N, 23.63. Found: C, 30.23; H, 3.14; N, 23.69%. Anal. calcd for $C_{24}H_{46}Co_2N_{12}O_{22}S_2$ (**3**): C, 27.81; H, 4.47; N, 16.21. Found: C, 27.61; H, 4.59; N, 16.12%.

The position and shape of the ring stretching modes of coordinated bipym in the case of **1** (1575vs and 1560sh cm^{-1}) and in **2** (1585sh, 1581vs, 1570m cm^{-1}) and **3** (1585sh, 1577vs and 1561m cm^{-1}) are consistent with the occurrence of only bridging bipym in the former[14] and of both terminal and bridging bipym in the two latter.[7,15]

Crystal structure determination and refinement

Crystals of dimensions 0.11 × 0.14 × 0.18 (**1**), 0.38 × 0.24 × 0.42 mm (**2**) and 0.38 × 0.22 × 0.16 mm (**3**) were mounted on a Siemens R3m/V automatic four-circle diffractometer and used for data collection. Diffraction data were collected

Table 2 Selected interatomic distances (Å) and angles (°) for compound **1** with e.s.d.s in parentheses[a]

Co(1)—N(1)	2.177(5)	Co(1)—N(3)	2.176(5)
Co(1)—O(1)	2.053(5)	Co(1)—O(2)	2.046(5)
Co(1)—N(2a)	2.172(5)	Co(1)—N(4b)	2.169(5)
N(1)—Co(1)—N(3)	171.8(2)	N(1)—Co(1)—O(1)	93.8(2)
N(3)—Co(1)—O(1)	92.6(2)	N(1)—Co(1)—O(2)	89.8(2)
N(3)—Co(1)—O(2)	95.1(2)	O(1)—Co(1)—O(2)	91.7(2)
N(1)—Co(1)—N(2a)	75.9(2)	N(3)—Co(1)—N(2a)	99.7(2)
O(1)—Co(1)—N(2a)	84.3(2)	O(2)—Co(1)—N(2a)	164.8(2)
N(1)—Co(1)—N(4b)	97.9(2)	N(3)—Co(1)—N(4b)	75.7(2)
O(1)—Co(1)—N(4b)	168.3(2)	O(2)—Co(1)—N(4b)	88.5(2)
N(2a)—Co(1)—N(4b)	98.4(2)		

Hydrogen bonds

A	D	H	A···D	A···H—D
O(8)	O(1)	H(2w)	2.68(1)	175(5)
O(8′)	O(1)	H(5w)	2.78(1)	160(4)
O(4)	O(2)	H(3w)	2.73(1)	160(7)
O(6c)	O(2)	H(4w)	2.79(2)	164(5)
O(7′c)	O(2)	H(4w)	2.87(3)	132(5)

[a] Symmetry codes: (a) $-x, -y, -z$; (b) $1-x, -y, -z$; (c) $-x, -y, 1-z$.

at room temperature by using graphite monochromated Mo-Kα radiation ($\lambda = 0.71073$ Å) with the $\omega-2\theta$ scan method. The unit cell parameters were determined from least-squares refinement of the setting angles of 25 reflections in the 2θ range of 15–30°. Information concerning crystallographic data collection and structure refinements is summarized in Table 1. Examination of two standard reflections, monitored after every 98 reflections, showed no sign of crystal deterioration. Lorentz polarization, extinction and absorption corrections[16] were applied to the intensity data.

The structures were solved by standard Patterson methods and subsequently completed by Fourier recycling. On the difference map of compound **1**, several oxygen positions were localized because of different coexisting orientations of one nitrate group. This disorder was described by assigning population parameters of 0.5 to each pair of sites. All non-hydrogen atoms were refined anisotropically. The hydrogen atoms of the water molecules were located on a ΔF map and refined with constraints. The hydrogen atoms of bipym were set in calculated positions and refined as riding atoms with a common fixed isotropic thermal parameter. Full-matrix least-squares refinement was carried out by minimizing the function $\Sigma\, w(|F_o| - |F_c|)^2$. Models reached convergence with values of the R and R_w indices listed in Table 1. Criteria for satisfactory

Table 3 Selected interatomic distances (Å) and angles (°) for compound **2** with e.s.d.s in parentheses[a]

Co(1)—N(1)	2.140(2)	Co(1)—N(3)	2.125(2)
Co(1)—N(5)	2.144(2)	Co(1)—O(1)	2.049(2)
Co(1)—O(2)	2.068(2)	Co(1)—N(6a)	2.159(2)
N(1)—Co(1)—N(3)	77.2(1)	N(1)—Co(1)—N(5)	169.5(1)
N(3)—Co(1)—N(5)	97.3(1)	N(1)—Co(1)—O(1)	96.3(1)
N(3)—Co(1)—O(1)	173.4(1)	N(5)—Co(1)—O(1)	89.1(1)
N(1)—Co(1)—O(2)	96.3(1)	N(3)—Co(1)—O(2)	87.3(1)
N(5)—Co(1)—O(2)	92.3(1)	O(1)—Co(1)—O(2)	94.2(1)
N(1)—Co(1)—N(6a)	93.7(1)	N(3)—Co(1)—N(6a)	87.9(1)
N(5)—Co(1)—N(6a)	77.1(1)	O(1)—Co(1)—N(6a)	91.8(1)
O(2)—Co(1)—N(6a)	167.7(1)		

Hydrogen bonds

A	D	H	A···D	A···H—D
O(5)	O(1)	H(1w)	2.78(1)	150(2)
O(9)	O(1)	H(2w)	2.62(1)	167(3)
O(7)	O(2)	H(4w)	2.75(1)	156(2)
O(8b)	O(9)	H(6w)	2.87(2)	168(3)

[a] Symmetry codes: (a) $-x, -y, 1-z$; (b) $-x, 1-y, -z$.

Table 4 Selected interatomic distances (Å) and angles (°) for compound **3** with e.s.d.s in parentheses[a]

Co(1)—N(1)	2.155(2)	Co(1)—N(3)	2.131(2)
Co(1)—N(5)	2.146(2)	Co(1)—O(1)	2.093(2)
Co(1)—O(2)	2.031(2)	Co(1)—N(6a)	2.157(2)
N(1)—Co(1)—N(3)	76.1(1)	N(1)—Co(1)—N(5)	97.4(1)
N(3)—Co(1)—N(5)	173.5(1)	N(1)—Co(1)—O(1)	93.4(1)
N(3)—Co(1)—O(1)	89.3(1)	N(5)—Co(1)—O(1)	91.6(1)
N(1)—Co(1)—O(2)	165.7(1)	N(3)—Co(1)—O(2)	90.3(1)
N(5)—Co(1)—O(2)	96.2(1)	O(1)—Co(1)—O(2)	90.8(1)
N(1)—Co(1)—N(6a)	88.2(1)	N(3)—Co(1)—N(6a)	102.0(1)
N(5)—Co(1)—N(6a)	77.0(1)	O(1)—Co(1)—N(6a)	168.6(1)
O(2)—Co(1)—N(6a)	90.5(1)		

Hydrogen bonds

A	D	H	A···D	A···H—D
O(4)	O(6)	H(3w)	2.69(1)	164(1)
O(6)	O(7)	H(5w)	2.76(1)	176(1)
O(3)	O(8)	H(7w)	2.72(1)	170(1)
O(4)	O(9)	H(9w)	2.79(1)	170(1)
O(5)	O(11)	H(13w)	2.80(1)	170(1)
O(7b)	O(8)	H(8w)	2.86(1)	179(1)
O(6c)	O(1)	H(1w)	2.70(1)	174(1)
O(8c)	O(1)	H(2w)	2.73(1)	173(1)
O(9d)	O(11)	H(14w)	2.79(1)	163(1)
O(10e)	O(7)	H(6w)	2.84(1)	163(1)
O(11f)	O(10)	H(11w)	2.75(1)	173(1)

[a] Symmetry codes: (a) $1-x, -y, -z$; (b) $0.5-x, 0.5+y, 0.5-z$; (c) $0.5-x, y-0.5, 0.5-z$; (d) $1.5-x, y-0.5, 0.5-z$; (e) $x-0.5, 0.5-y, 0.5+z$; (f) $1.5-x, 0.5+y, 0.5-z$.

complete analysis were the ratios of the root mean square shift to standard deviation being less than 0.011 and no significant features in final difference maps. Solutions and refinements were performed with the SHELXTL-PLUS system.[17] The final geometrical calculations were carried out with the PARST program.[18] The graphical manipulations were performed using the XP utility of the SHELXTL-PLUS system. Main interatomic bond distances and angles are listed in Tables 2 (**1**), 3 (**2**) and 4 (**3**).

CCDC reference number 440/015.

Results and Discussion

Description of the structures

Crystal structure of 1. The structure of complex **1** consists of cationic chains of cobalt(II) ions bridged by bipym molecules, coordinated water molecules and uncoordinated nitrate anions. An extensive network of hydrogen bonds (see end of Table 2) involving oxygen atoms of both coordinated and uncoordinated water molecules and nitrate groups occurs. A perspective view of the cationic chain of **1** is shown in Fig. 1. Inversion centres are located at the middle of the C(4)—C(4a) and C(8)—C(8b) bonds of the bipym molecules, which are not equivalent. Neighbouring chains are well separated from each other, the shortest interchain metal–metal separation being 7.632(2) Å [Co(1)···Co(1d) with (d) $= 1-x, -y, 1-z$]. This structure is similar to that reported for the parent Mn^{II},[8] Fe^{II} [19] and Cu^{II} [20] chains and it constitutes the first example of a bipym-bridged Co^{II} chain.

Each cobalt atom is in a distorted octahedral environment, being bonded to four nitrogen atoms of bipym and two oxygen atoms of water in a *cis* position. The Co—N bond distances [ave. value is 2.173(5) Å] are much longer than the Co—O ones [ave. value is 2.049(5) Å], but they are shorter than that observed for Mn—N(bipym) and Fe—N(bipym) in the related $[Mn(bipym)(NCO)_2]$[8] (ave. value 2.35 Å) and $[Fe(bipym)(NCS)_2]$[19] (ave. value 2.24 Å) chains, as expected. The main distortion from the octahedral symmetry of the

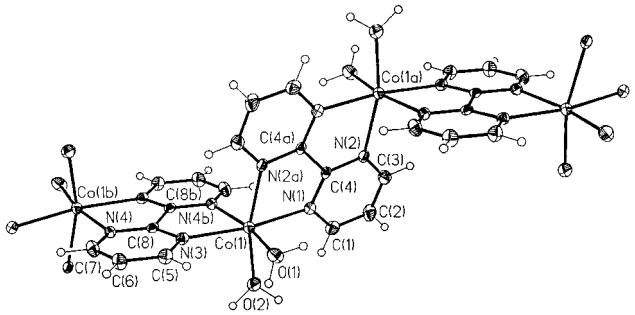

Fig. 1 Perspective drawing of a fragment of the cationic $[Co(bipym)(H_2O)_2]^{2+}$ unit in **1** showing the atom numbering. Thermal ellipsoids are drawn at the 30% probability level

metal environment is due to the bite angles of the coordinated bipym [(ave. value is 75.8(2)°]. The best equatorial plane is defined by the N(1), N(3), N(4), O(1) atoms [largest deviation from the mean plane is 0.056(5) Å for N(4b)]. The cobalt atom is 0.045(1) Å out of this plane. The pyrimidyl rings are planar, as expected, with deviations not greater than 0.013(6) Å from the mean planes. The bipym ligand as a whole is planar. The Co(1) atom is 0.128(1) and 0.068(1) Å out of the bipym planes containing the N(1) and N(3) atoms, respectively. The dihedral angle between the mean adjacent bipym planes is 76.7(2)°.

The metal–metal separations across the bridging bipym are 5.794(2) and 5.808(2) Å for Co(1)···Co(1a) and Co(1)···Co(1b), respectively. The nitrate anion has its expected planar trigonal geometry. The nitrogen–oxygen bond lengths and the intra-anion bond angles average 1.24(2) Å and 120(2)°, respectively. However, the values of two bond angles deviate significantly from the ideal value [113.0(12) and 125.9(13)° for O(6)—N(6)—O(8) and O(7)—N(6)—O(8), respectively].

Crystal structures of 2 and 3. The structures of compounds **2** and **3** consist of centrosymmetric dinuclear units where both chelating and bis(chelating) bipym groups are present, together with coordinated and crystallization water molecules. Electroneutrality is achieved by noncoordinated nitrate (**2**) and monodentate sulfate anions (**3**). The molecular geometries with the atom labelling schemes for **2** and **3** are shown in Fig. 2 and 3, respectively. Two water molecules of crystallization in **2** and twelve in **3** contribute to the packing by forming an extensive network of hydrogen bonds (see end of Tables 2 and 3) in which oxygen atoms of coordinated and noncoordinated water molecules as well as from nitrate (**2**) and sulfate (**3**) groups are involved.

Each cobalt atom is linked to four nitrogen atoms of two bipym molecules, one acting as an end-cap ligand and the other one as a bridge. The distorted octahedral coordination

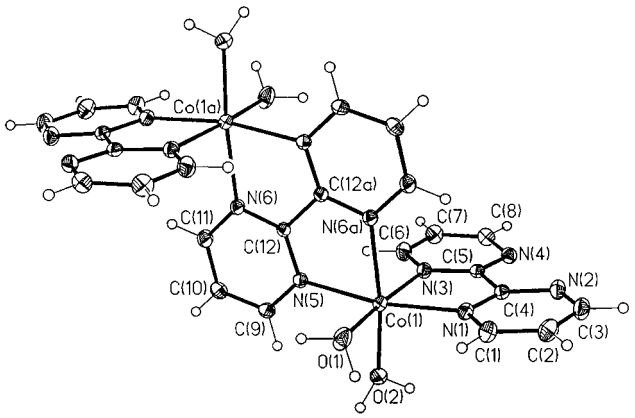

Fig. 2 Perspective view of the cationic $[Co_2(bipym)_3(H_2O)_4]^{4+}$ unit of complex **2** showing the atom numbering. Thermal ellipsoids are drawn at the 30% probability level

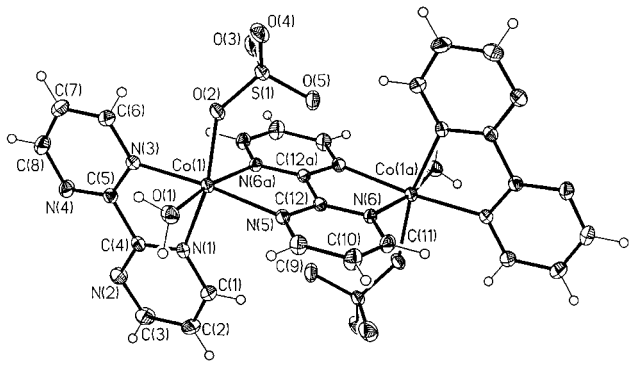

Fig. 3 Perspective drawing of complex **3** showing the atom numbering. The crystallization water molecules have been omitted for clarity. Thermal ellipsoids are drawn at the 30% probability level

around the metal atom is reached by means of two coordinated water molecules in a *cis* position (**2**), or a water molecule and an oxygen atom from a monodentate sulfate (**2**). The Co—N bond lengths average 2.142(2) (**2**) and 2.147(2) Å (**3**) and they are longer than the Co—O ones. [ave. value of 2.058(2) in **2** and 2.093(2) and 2.031(2) Å, this last for the oxygen from sulfate, in **3**]. The structures of **2** and **3** are similar to that of the complex $[Co_2(bpm)_3(NCS)_4]$ (**4**).[14] No relevant differences in the bond distances of the organic ligand were found. However, the metal–metal intramolecular separation is shortened from 5.942°(2) Å in **4** to 5.73(2) Å in **2** and 5.737(1) Å in **3** because of the decrease in the Co—N (bridging bipym) distances when going from **4** to **2** and **3**. Consequently, the values of the bite angle of the bridging bipym in **2** [77.1(1)°] and **3** [77.0(1)°] are greater than that in **4** [73.7(1)°]. The value of the bite angle at the terminal bipym [77.2(1) and 76.1(1)° for **2** and **3**] are very close to that of the bridging bipym. The best equatorial plane is defined by the N(5), N(6a), N(1), O(2) atoms for **2** and the N(3), O(2), N(1), N(5) atoms for **3** [the largest deviation from the mean plane is 0.010(2) Å for N(5) (**2**), and 0.039(2) Å for N(3) (**3**)]. The cobalt atom is displaced from these planes by 0.113(1) Å (**2**) and 0.048(1) Å (**3**).

All pyrimidyl rings are planar, with deviations from the mean planes not greater than 0.014(2) (**2**) and 0.007(2) (**3**) Å (bridging bipym), and 0.013(2) (**2**) and 0.011(4) (**3**) Å (terminal bipym). In the terminal bipym groups the two pyrimidine rings form a dihedral angle of 5.3(1)° (**2**) and 1.6(1)° (**3**), whereas they are coplanar in the central bipym. The nitrate and sulfate anions have their expected trigonal and tetrahedral geometries, respectively. The nitrogen–oxygen bond lengths and the intra-anion bond angles average to 1.234(4) Å and 119.9(3)°, respectively. The average sulfur–oxygen bond distance and intra-ion bond angle for the sulfate group are 1.470(3) Å and 109.5(1)°.

The arrangement of the dinuclear units in complexes **2** and **3** shows linear chains connected by graphitic interactions between the terminal bipyms. This arrangement is identical to that previously reported for complex **4** [the distance between the facing rings is 3.341(2) Å in **2**, 3.319(3) Å in **3** and 3.378(3) Å in **4**]. The resulting linear chains are connected by hydrogen bonds and van der Waals interactions. The shortest intermolecular metal–metal separation is 7.580(1) Å [Co(1)···Co(1c) with (c) = $-x$, $-y$, $-z$] (**2**) and 7.463(1) Å [Co(1)···Co(1c) with (c) = $0.5 - x$, $y - 0.5$, $0.5 - z$] (**3**).

Magnetic properties of 1–3

The magnetic properties of the dinuclear complexes **2** and **3** in the form of plots of both χ_M (molar magnetic susceptibility) and $\chi_M T$ *vs.* T are shown in Fig. 4 and 5, respectively. The susceptibility curves show maxima at 14 (**2**) and 13.5 K (**3**), whereas the $\chi_M T$ curves exhibit a continuous decrease upon cooling, with $\chi_M T = 5.75$ (μ_{eff} per $Co^{II} = 4.80$ μ_B) (**2**) and 5.30

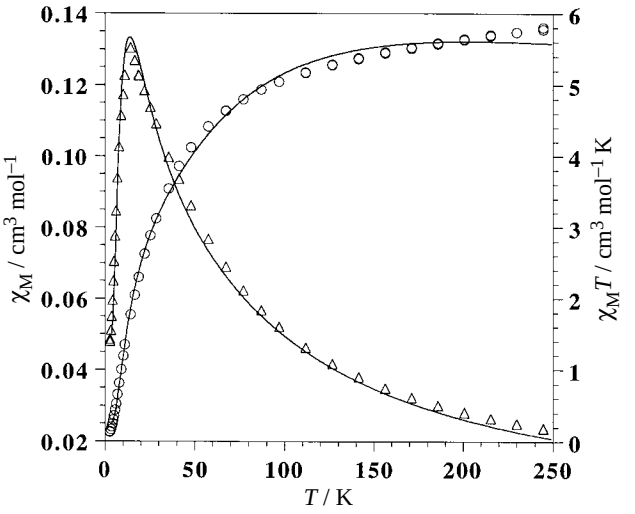

Fig. 4 Thermal dependence of the molar magnetic susceptibility χ_M (△) and $\chi_M T$ (○) for complex **2**. The solid line corresponds to the best fit through the Lines approach (see text)

cm^3 mol^{-1} K (4.60 μ_B) (**3**) at 290 K and an extrapolated value that vanishes when T approaches zero. The presence of a maximum in the susceptibility curve is indicative of an antiferromagnetic interaction between the metal centres with a singlet ground state. In addition, the fact that the values of μ_{eff} per metal atom at room temperature are larger than that expected for the spin-only case (3.87 μ_B $S = 3/2$) reveals that a significant orbital contribution is involved.

The analysis of the susceptibility data of the dinuclear complexes **2** and **3** through the spin-only formalism [eqn. (1)]

$$\hat{H} = -J\hat{S}_A \cdot \hat{S}_B \quad (1)$$

implying an isotropic Heisenberg interaction with $S_A = S_B = 3/2$ was unsuccessful because the distortion of the octahedral symmetry of Co^{II} is not so important as to induce total quenching of the orbital momentum of the $^4T_{1g}$ ground state. The calculated χ_M curves do not match well the experimental data in the vicinity of the maximum, the position of the theoretical maximum being shifted toward higher temperatures with respect to that of the experimental one. The values of the magnetic coupling J thus obtained (−7.7 and −7.1 cm^{-1} for **2** and **3**, respectively) are overestimated and they should be significantly reduced by taking into account the orbital reduction factor x and the spin-orbit coupling parameter λ. The Lines theory[21] of polynuclear compounds of Co^{II} allows this treatment, the corresponding susceptibility expression for a Co^{II} dimer is given in eqn. (2)

$$\chi_M = \{2N\beta^2[g(T)]^2/kT\}[3 + \exp(-25J/9kT)]^{-1} \quad (2)$$

The parameters N, β and k have their usual meanings whereas $g(T)$ is a temperature-dependent g factor, which needs to be evaluated for each T value in order to generate the theoretical χ_M *vs.* T curve.[14,21] The computed susceptibility curves for complexes **2** and **3** through eqn. (2) matched quite well the experimental data as shown in Fig. 4 and 5. The values of the parameters J, λ, x and R obtained by least-squares minimization are −5.4 cm^{-1}, −103 cm^{-1}, 0.79 and 7.4 × 10^{-4} for **2** and −5.1 cm^{-1}, −110 cm^{-1}, 0.63 and 7.9 × 10^{-4} for **3**, respectively; R is the agreement factor defined as $\Sigma[(\chi_M)_{obs} - (\chi_M)_{calc}]^2/\Sigma[(\chi_M)_{obs}]^2$. Finally, assuming that only the Kramer's doublet for Co^{II} remains populated for $T < 30$ K, we have analyzed the low temperature susceptibility data ($2.5 < T < 30$ K) of complexes **2** and **3** through the corresponding expression for χ_M involving two spin doublets (Ising dimer, $S_{eff} = 1/2$).[22] It is satisfying to point out that the values obtained for J are practically identical to that determined through the Lines approach and they are very close to that reported for parent bipym-bridged Co^{II} dinuclear complexes.[14]

The magnetic properties of the infinite linear chain **1** as χ_M and $\chi_M T$ *vs.* T plots are shown in Fig. 6 for $T < 150$ K. The $\chi_M T$ curve exhibits a continuous decrease upon cooling, with $\chi_M T = 2.7$ cm^3 mol^{-1} K (μ_{eff} per Co^{II} = 4.65 μ_B) at 290 K and a value very close to zero at 2.5 K. The susceptibility curve shows a rounded maximum at 18 K. These features are characteristic of the occurrence of a relatively important intrachain antiferromagnetic coupling between the high-spin cobalt(II) ions. In a first approach, we have attempted to reproduce theoretically the experimental susceptibility by using the classical spin Heisenberg chain model[23] through the Hamiltonian [eqn. (3)]

$$\hat{H} = -J\sum \hat{S}_i \cdot \hat{S}_{i+1} \quad (3)$$

The parameters J, g and R obtained by least-squares minimization were −8.5 cm^{-1}, 2.54 and 5 × 10^{-4}, respectively. The position of the calculated susceptibility maximum for **1** is shifted towards higher temperature with respect to that of the experimental curve for the same reasons outlined above in the case of fits concerning complexes **2** and **3**. Given that only the Kramer's doublet for Co^{II} is populated at $T < 30$ K, we have analyzed the magnetic data in the temperature range

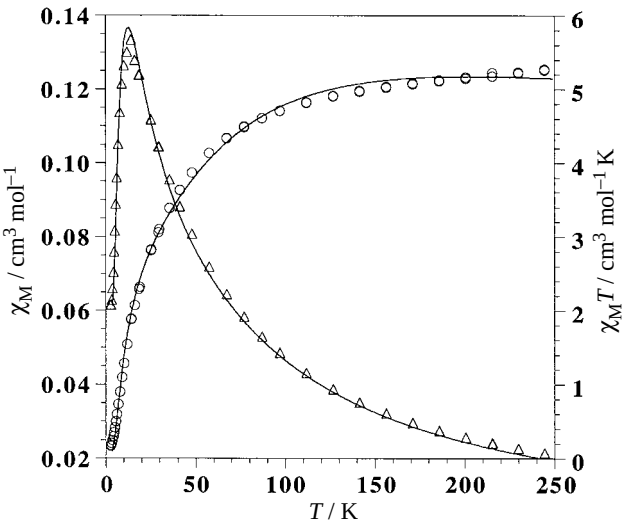

Fig. 5 Thermal dependence of the molar magnetic susceptibility χ_M (△) and $\chi_M T$ (○) for complex **3**. The solid line corresponds to the best fit through the Lines approach (see text)

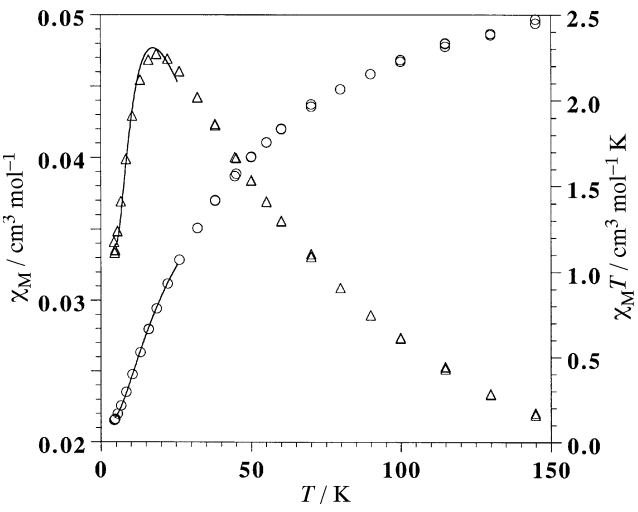

Fig. 6 Thermal dependence of the molar magnetic susceptibility χ_M (△) and $\chi_M T$ (○) for complex **1**. The solid line in the temperature range 2.5–30 K corresponds to the best fit through the Ising model (see text)

Table 5 Selected magnetostructural data for bipym-bridged complexes with first-row transition metal ions[a]

Compound	Nuclearity	$d_{M-N(bipym)}$/Å[b]	$d_{M\cdots M}$/Å[c]	$-J$/cm^{-1} [d]	$n_A n_B J$/cm^{-1}	Ref
$[Mn(bipym)(NCO)_2]$	chain	2.35	6.23	1.1	27.5	5, 8
$[Mn(bipym)(NO_3)_2]$	chain	2.36	6.24	0.93	23.3	8
$[Fe(bipym)(NCS)_2]$	chain	2.24	5.96	3.5	56	19
1	chain	2.17	5.80	5.6	50.4	this work
$[Cu(bipym)(H_2O)_2](ClO_4)_2 \cdot H_2O$	chain	2.04(2.18)	5.60	62	62	20
$[Mn_2(bipym)_3(NCS)_4]$	dimer	2.36	6.22	1.19	29.8	7
$[Mn_2(bipym)(H_2O)_6(SO_4)_2]$	dimer	2.31	6.12	1.1	27.5	6
$[Fe_2(bipym)_3(NCS)_4]$	dimer	2.27	6.05	4.1	65.6	25
$[Fe_2(bipym)(H_2O)_6(SO_4)_2]$	dimer	2.22	5.91	3.1	41.6	26
$[Fe_2(bipym)(H_2O)_8](SO_4)_2 \cdot 2H_2O$	dimer	2.22	5.84	3.4	54.4	26
$[Co_2(hfa)_4(bipym)]$	dimer	2.15	5.75	7.0	63.0	27
$[Co_2(bipym)(H_2O)_8](NO_3)_4$	dimer	2.16	5.76	5.4	48.6	14
$[Co_2(bipym)(H_2O)_8](SO_4)_2 \cdot 2H_2O$	dimer	2.17	5.78	4.7	42.3	14
$[Co_2(bipym)_3(NCS)_4]$	dimer	2.23	5.94	6.2	55.8	14
2	dimer	2.14	5.74	5.4	48.6	this work
3	dimer	2.15	5.74	5.1	45.9	this work
$[Cu_2(bipym)(C_5O_5)_2(H_2O)_2] \cdot 4H_2O$	dimer	2.02	5.38	160	160	28
$[Cu_2(bipym)(C_4O_4)_2(H_2O)_6]$	dimer	2.07	5.54	139	139	29
$[Cu_2(bipym)(H_2O)_4(SO_4)_2] \cdot 3H_2O$	dimer	2.04	5.46	159	159	30

[a] Abbreviations used: hfa = hexafluoroacetylacetonate, $C_5O_5^{2-}$ = dianion of croconic acid; $C_4O_4^{2-}$ = dianion of squaric acid. [b] Average value for the metal-to-nitrogen (bridging bipym) bond. [c] Metal–metal separation across bipym. [d] Exchange interaction through bridging bipym.

$2.5 < T < 30$ K through the Ising model for a chain of interacting spins $S_{eff} = 1/2$.[24] The values of the parameters J, $g_{\|}$, $g_{\perp}$ and R are -5.6 cm^{-1}, 8.3, 1.1 and 2×10^{-4}, respectively. A satisfactory match of the experimental data in the low temperature region is obtained through this approach, as shown in Fig. 6.

The values of the antiferromagnetic coupling through bridging bipym in the complexes **1**–**3** are very close, as expected in the light of their structural similarities, and they lie within the range reported for other bipym-bridged Co^{II} complexes.[14] The significant σ in-plane overlap between the two metal-centred $d_{x^2-y^2}$ type magnetic orbitals through bridging bipym in the dimers **2** and **3** accounts mainly for this antiferromagnetic coupling.[3]

It is interesting to examine the variation of the magnitude of the magnetic coupling in the bipym-bridged chains as a function of the size of the local interacting spins. This information is summarized in Table 5 together with that concerning parent dimers. The inclusion of the values of $n_A n_B J$ in this table ($n_A = n_B$ = number of unpaired electrons on two adjacent metal centres) is due to the fact that the magnitude of the antiferromagnetic interaction is properly described not by J, but by $n_A n_B J$.[31] In the light of the magneto-structural data listed therein, two main points deserve comment: (i) the values of $-J$ for the Mn^{II}, Fe^{II} and Co^{II} chains are in agreement with those reported for the corresponding bipym-bridged dinuclear compounds as expected, whereas that of the Cu^{II} chain (62 cm^{-1}) is too low when compared to the observed value in the related bipym-bridged copper(II) dimers (see the three last entries in Table 5); (ii) the values of $-n_A n_B J$ should increase when going from Mn^{II} to Cu^{II} but for the Fe^{II} and Co^{II} compounds they are very close. Dealing with the first point, this discrepancy has a structural origin. In fact, in the last compound of Table 5 the two $d_{x^2-y^2}$ magnetic orbitals of the two Cu^{II} ions are in the plane of the bridging bipym [the x and y axes being roughly defined by the Cu—N(bipym) bonds] and consequently, they overlap through the two NCN pyrimidyl bridging skeletons in contrast to the Cu^{II} chain where the adjacent $d_{x^2-y^2}$ magnetic orbitals are turned by 90°, the overlap occurring only through one of the NCN fragments. This phenomenon, which is referred to as orbital reversal,[20b,32] accounts for the reduction of the magnitude of the antiferromagnetic coupling in the copper(II) chain. The usual value of $-J$ for bipym-bridged copper(II) complexes when the magnetic orbitals are coplanar with bipym is around 200 cm^{-1}, lower values being observed because of different factors such as structural distortions,[29] symmetry changes of the interacting magnetic orbitals[30,20b] and the different electronegativity of the peripheral donor atoms.[33] As far as the second point is concerned, it is clear that the energy of the 3d orbitals decreases when going from Mn^{II} to Cu^{II} and so, the energy gap between these orbitals and that of the symmetry-adapted HOMOs of the bipym becomes smaller when going from Mn^{II} to Cu^{II} compounds. The result is a greater contribution of the bridging bpym ligand orbitals to the magnetic orbitals for Cu^{II} than for Mn^{II}. This induces a better overlap between the magnetic orbitals in Cu^{II} dimers than in Mn^{II} dimers, resulting in a stronger antiferromagnetic interaction in the former. However, the fact that the value of $-n_A n_B J$ for the Fe^{II} and Co^{II} cases does not follow the expected trend reveals that the energy of the 3d orbitals is not the only factor to be considered. In a previous contribution,[7] we have noted that the ligand field effects cannot be disregarded when analyzing the magnetic behaviour of the bipym-containing complexes: the value of 10Dq for bipym complexes with Fe^{II} and Co^{II} is very close, indicating that a similar metal–ligand interaction is involved, leading most likely to a similar spin delocalization on the bridge and thus, to a close magnetic coupling. In addition, the spin-only formalism was used to determine the J value in the Fe^{II} complexes and, given that the orbital contribution is most likely significant in this type of compound, the magnitude of the exchange coupling reported is an upper limit. This overestimation of the J value is clearly illustrated by the family of Co^{II} dimers in Table 5. The somewhat greater value for $-J$ of the hfa derivative is due to the fact that it was determined by using a spin-only expression, in contrast to what was done for the other compounds.

The present work shows that the exchange coupling values determined for the chain compounds with different first-row transition metal ions are in agreement with those reported for the corresponding dimeric systems. This feature is to be taken into account when analyzing the magnetic properties of much more complicated higher dimensionality magnetic systems, which are more and more common in the literature.

Acknowledgements

This work was supported by the Spanish DGICYT (Project PB94-1002) and the Italian Ministero dell'Università e della

Ricerca Scientifica e Technologica. G. V. thanks the Spanish Ministery of Education and Science for a postdoctoral fellowship. We are very indebted to Dr. A. Caneschi (University of Firenze, Italy) for recording the variable-temperature magnetic susceptibility data for complexes **1**–**3**.

References

1 G. De Munno and M. Julve, in *Metal-Ligand Interactions. Structure and Reactivity*, ed. N. Russo and D. R. Salahub, Kluwer, Dordrecht, 1996, p. 139.
2 G. De Munno, F. Lloret and M. Julve, in *Magnetism: A Supramolecular Function*, ed. O. Kahn, Kluwer, Dordrecht, 1996, p. 555.
3 M. Julve, G. De Munno, G. Bruno and M. Verdaguer, *Inorg. Chem.*, 1988, **27**, 3160.
4 R. R. Ruminski and J. D. Petersen, *Inorg. Chim. Acta*, 1985, **97**, 129.
5 D. M. Hong, H. H. Wei, L. L. Gan, G. H. Lee and Y. Wang, *Polyhedron*, 1996, **15**, 2335.
6 G. De Munno, R. Ruiz, F. Lloret, J. Faus, R. Sessoli and M. Julve, *Inorg. Chem.*, 1995, **34**, 408.
7 G. De Munno, G. Viau, M. Julve, F. Lloret and J. Faus, *Inorg. Chim. Acta*, 1997, **257**, 121.
8 G. De Munno, T. Poerio, M. Julve, F. Lloret, G. Viau and A. Caneschi, *J. Chem. Soc., Dalton Trans.*, 1997, 601.
9 (a) G. De Munno, M. Julve, G. Viau, F. Lloret, J. Faus and D. Viterbo, *Angew. Chem., Int. Ed. Engl.*, 1996, **35**, 1807; (b) R. Cortés, L. Lezama, J. L. Pizarro, M. I. Arriortua and T. Rojo, *ibid.*, 1996, **35**, 1810.
10 (a) G. De Munno, M. Julve, F. Lloret, J. Faus, M. Verdaguer and A. Caneschi, *Angew. Chem., Int. Ed. Engl.*, 1993, **32**, 1045; (b) G. De Munno, M. Julve, F. Lloret, J. Faus, M. Verdaguer and A. Caneschi, *Inorg. Chem.*, 1995, **34**, 157.
11 G. De Munno, M. Julve, F. Nicoló, F. Lloret, J. Faus, R. Ruiz and E. Sinn, *Angew. Chem., Int. Ed. Engl.*, 1993, **32**, 613.
12 G. De Munno, T. Poerio, G. Viau, M. Julve, F. Lloret, Y. Journaux and E. Rivière, *Chem. Commun.*, 1996, 2587.
13 A. Earshaw, *Introduction to Magnetochemistry*, Academic, London and New York, 1968.
14 M. Julve, M. Verdaguer, G. De Munno, J. A. Real and G. Bruno, *Inorg. Chem.*, 1993, **32**, 795.
15 G. De Munno, M. Julve, F. Lloret, J. Faus and A. Caneschi, *J. Chem. Soc., Dalton Trans.*, 1994, 1175.
16 A. C. T. North, D. C. Phillips and F. S. Mathews, *Acta Crystallogr., Sect. A*, 1968, **24**, 351.
17 G. M. Sheldrick, *SHELXTL-PLUS Crystallographic System*, Release 4.21/V, Siemens Analytical X-ray Instruments, Madison, WI, 1990.
18 M. Nardelli, *Comput. Chem.*, 1983, **7**, 95.
19 G. De Munno, M. Julve, J. A. Real, F. Lloret and R. Scopellitti, *Inorg. Chim. Acta*, 1996, **250**, 81.
20 (a) L. W. Morgan, K. V. Goodwin, W. T. Pennington and J. D. Petersen, *Inorg. Chem.*, 1992, **31**, 1103; (b) G. De Munno, M. Julve, M. Verdaguer and G. Bruno, *ibid.*, 1993, **32**, 2215.
21 M. E. Lines, *J. Chem. Phys.*, 1971, **55**, 2977.
22 E. Coronado, M. Drillon, P. R. Nugteren, L. J. de Jongh and D. Beltrán, *J. Am. Chem. Soc.*, 1988, **110**, 3907.
23 (a) H. Fisher, *Am. J. Phys.*, 1964, **32**, 343; (b) G. R. Wagner and S. A. Friedberg, *Phys. Lett.*, 1964, **9**, 11.
24 M. E. Fisher, *J. Math. Phys.*, 1963, **4**, 124.
25 J. A. Real, J. Zarembowitch, O. Kahn and X. Solans, *Inorg. Chem.*, 1987, **26**, 2939.
26 E. Andrés, G. De Munno, M. Julve, J. A. Real and F. Lloret, *J. Chem. Soc., Dalton Trans.*, 1993, 2169.
27 G. Brewer and E. Sinn, *Inorg. Chem.*, 1985, **24**, 4580.
28 I. Castro, J. Sletten, L. K. Glærum, F. Lloret, J. Faus and M. Julve, *J. Chem. Soc., Dalton Trans.*, 1994, 2777.
29 I. Castro, J. Sletten, L. K. Glærum, J. Cano, F. Lloret, J. Faus and M. Julve, *J. Chem. Soc., Dalton Trans.*, 1995, 3207.
30 G. De Munno, M. Julve, F. Lloret, J. Cano and A. Caneschi, *Inorg. Chem.*, 1995, **34**, 2048.
31 O. Kahn, *Struct. Bonding (Berlin)*, 1987, **68**, 89 and references cited therein.
32 J. J. Girerd, O. Kahn and M. Verdaguer, *Inorg. Chem.*, 1980, **19**, 274.
33 P. Román, C. Guzmán-Miralles, A. Luque, J. I. Beitia, J. Cano, F. Lloret, M. Julve and S. Alvarez, *Inorg. Chem.*, 1996, **35**, 3741.

Received 22nd May 1997; *revised M/S received* 18*th August* 1997; *Paper* 7/08329G